Journal of Power Sources 196 (2011) 5803–5810

Contents lists available at ScienceDirect

Journal of Power Sources

journal homepage: www.elsevier.com/locate/jpowsour

Hybrid proton conducting membranes based on sulfonated cross-linked polysiloxane network for direct methanol fuel cell

Jing Zhu[a], Gang Zhang[a], Ke Shao[b], Chengji Zhao[a], Hongtao Li[a], Yang Zhang[a], Miaomiao Han[a], Haidan Lin[a], Mu Li[a], Hui Na[a,*]

[a] Alan G MacDiarmid Institute, College of Chemistry, Jilin University, Qianjin Street 2699#, Changchun, Jilin 130012, People's Republic of China
[b] Institute of Urban Environment Chinese Academy of Sciences, Xiamen 361021, People's Republic of China

ARTICLE INFO

Article history:
Received 24 January 2011
Received in revised form 9 March 2011
Accepted 9 March 2011
Available online 17 March 2011

Keywords:
Hybrid
Cross-linked
Sulfonated
Proton exchange membrane

ABSTRACT

A series of novel hybrid membranes based on sulfonated poly(arylene ether ketone)s (SNPAEKs), polysiloxane (KH-560) and sulfonated curing agent (BDSA) has been prepared by sol–gel and cross-linking reaction for direct methanol fuel cells (DMFCs). All the hybrid membranes (SKB-*xx*) show high thermal properties and improved oxidative stability compared with the pristine SNPAEK membrane. The sulfonated cross-linked polysiloxanes networks in the hybrid membranes enhance the mechanical properties and reduce the swelling ratio. The swelling ratio of SKB-20 is 22%, which is much lower than that of the pristine SNPAEK (37%) at 80 °C. Meanwhile, SKB-*xx* membranes with greatly reduced methanol permeabilities show comparative proton conductivities to pristine SNPAEK membranes. Notably, the proton conductivities of SKB-5 and SKB-10 reach to 0.192 S cm^{-1} and 0.179 S cm^{-1} at 80 °C, respectively, which are even higher than the 0.175 S cm^{-1} of SNPAEK.

1. Introduction

Direct methanol fuel cells (DMFCs) have recently received considerable attention as clean and efficient power sources for automotive, stationary, and portable applications [1,2]. Proton exchange membranes (PEMs) are employed as electrolyte in DMFCs. Current commercial proton exchange membranes based on perfluorosulfonic acid (PSFA), such as Nafion, show excellent chemical and mechanical stabilities as well as high proton conductivity at moderate temperatures (≦80 °C) and 100% relative humidity. However, the disadvantages of perfluorosulfonic acid polymers, such as high cost, environmental concerns of the fluorinated materials as well as excessive methanol permeability limit their commercialization in DMFCs [3,4]. The development of alternative PEMs with excellent stability, high proton conductivity and low methanol permeation is a major challenge.

During past years, sulfonated aromatic polymers have been widely investigated as candidate PEM materials for DMFCs applications because of their low methanol permeability, excellent thermal and chemical stabilities [5–9]. Main-chain-type sulfonated polymers with the sulfonic acid groups directly attached onto the polymer main chain typically show extensive water uptake above a critical temperature, or above a critical degree of sulfonation, which result in a dramatic loss of mechanical properties [10]. Many research groups found that the side-chain-type sulfonated aromatic polymers, which located the sulfonic acid groups on the side chains, exhibited pronounced hydrophilic/hydrophobic phase separation. Based on this, the side-chain-type sulfonated polymers possessed advantageous conductivity and membrane hydrodynamic properties compared to most of the main-chain-type sulfonated polymers [11,12]. In our previous work, we have prepared naphthalene-based poly(aryl ether ketone) copolymers containing sulfobutyl pendant groups(SNPAEK), which showed promising performance [13]. In general, the sulfonated aromatic polymer membranes require high degree of sulfonation (Ds) to achieve sufficient proton conductivity [14]. However, high Ds would lead to high water uptake and high swelling ratio, which result in the loss of the mechanical strength and the increase of the methanol permeability [15–17].

Organic–inorganic hybrid method has become an important approach in the modification of PEMs by combining the effects of organic polymers and inorganic compounds [18,19]. Cross-linking is another simple and powerful method to improve the dimensional stability and the methanol resistance of PEMs [20]. Chen and Kuo used the organic–inorganic hybrid method to modify the Nafion membranes, which incorporated hydrophilic polymer into covalently cross-linked polysiloxanes. The resulting hybrid membranes greatly decreased the methanol permeability

* Corresponding author. Tel.: +86 431 85168870; fax: +86 431 85168868.
E-mail address: huina@jlu.edu.cn (H. Na).

0378-7753/$ – see front matter © 2011 Elsevier B.V. All rights reserved.
doi:10.1016/j.jpowsour.2011.03.021

to 10^{-8} cm^2 s^{-1} [21]. However, the hybrid membranes showed a tendency toward decreased proton conductivity due to the reduction of ion exchange capacities (IECs) [22]. To overcome this problem, several sulfonic acid functionalized inorganic fillers such as sulfonated clays, sulfonated MCM-41 and sulfonated SBA-15 have been used to improve the proton conductivity of the hybrid membranes [23–25]. Lavorgna et al. have reported the hybrid membranes which introduced the sulfonic acid functionalized polysiloxane domains into Nafion membranes, and the presence of SO_3H-functionalized polysiloxane improved the proton conductivity of the hybrid membranes [26].

In this study, we demonstrate a novel hybrid membrane for DMFC by using a sulfonated curing agent to form polysiloxane cross-linked network. The hybrid membranes were composed of side-chain-type SNPAEK, 3-glycidoxypropyltrimethoxysilane (KH-560) and 2,2-benzidinedisulfonic acid (BDSA). In the hybrid membranes, the side-chain-type SNPAEK acts as the matrix which guarantees the high proton conductivity of the composite membranes. KH-560 can form the polysiloxane cross-linked structure to improve the mechanical and dimensional stability of the membranes, and the BDSA not only acts as curing agent but also provides additional proton conducting sites. The dimensional and oxidative stability of the resulting SNPAEK/KH-560/BDSA hybrid membranes have been investigated thoroughly. Also the methanol permeability and proton conductivity of these hybrid membranes were compared with the pristine SNPAEK membranes. All the results show that the hybrid membranes would be the promising PEMs materials in DMFCs.

2. Experimental

2.1. Materials

HNPAEK was synthesized by the aromatic nucleophilic polycondensation of 1,5-bis(4-fluorobenzoyl)-2,6-dimethoxynaphthalene(DMNF) and bisphenol A according to the procedure described in our previous work [27]. Then the HNPAEK was sulfobutylated by 1,4-butane sultone to form SNPAEK. The degree of sulfonation, which was defined as the molar ratio (%) of sulfonic acid groups converted from hydroxyl groups, was determined by the ^{1}H NMR method [28,29]. Fig. 1 shows the ^{1}H NMR spectrum of the SNPAEK. The degree of sulfonation was 96%, which was calculated from the ^{1}H NMR spectrum, in which the A_{H8} and A_{HAr} corresponded to the peak area of H_8 and H_{Ar}, respectively [27]. 2,2-Benzidinedisulfonic acid (BDSA) was purchased from TCI Co. and triethylamine was purchased from Shanghai Chemicals Co. BDSA was dissolved in ethanol and neutralized by adding triethylamine at 60 °C to form BDSA–Et_3HN. BDSA–Et_3HN was purified by recrystallization from ethanol solution and dried under vacuum for three days. Dimethyl sulfoxide (DMSO), which purchased from Beijing Chemical Co., was vacuum-distilled prior to use. Other reagents which purchased from Beijing Chemical Co. are all analytical reagent and used without further purification.

2.2. Preparation of the SKB-xx membranes

The hybrid membranes were prepared according to the following procedure. SNPAEK was dissolved in 10 mL dimethyl sulfoxide (DMSO) at room temperature to obtain 10 wt% solution. A certain weight of 3-glycidoxypropyltrimethoxysilane (KH-560) and BDSA–Et_3HN (KH-560/BDSA–Et_3HN = 4/1 mol/mol) were added to the SNPAEK solution, meanwhile, they were stirred for about 2 h. The homogeneous solution was cast on a 10 cm × 10 cm square aluminum plate and heated in a vacuum oven at 70 °C for 24 h to remove the DMSO completely and then at 150 °C for 1 h to accomplish the reaction between KH-560 and BDSA–Et_3HN. Dry membranes were peeled off from the substrate and immersed in 1 M H_2SO_4 solution at 80 °C for 24 h to get the KH-560 hydrolysis–condensation to happen, meanwhile the BDSA–Et_3HN in the membranes converted into the BDSA. SKB-*xx* were prepared subsequently, where *xx* represents the weight percentages of KH-560 in the hybrid membranes (*xx* = 5, 10, 15, 20). Meanwhile, the SK-10 which contained only 10 wt% KH-560 but no BDSA–Et_3HN was prepared for further comparison.

2.3. Characterization

^{1}H NMR spectrum was conducted with a 500 MHz Bruker Avance 510 spectrometer with deuterated dimethyl sulfoxide (DMSO-d_6) as the solvent and tetramethylsilane (TMS) as the standard. FT-IR spectroscopy measurements of the dry membrane samples were recorded from powder samples, which were scraped from the membranes by a bistoury and dispersed in dry KBr in form of disks, using a BRUKER Vector 22 spectrometer at a resolution of 4 cm^{-1} min^{-1} from 4000 to 400 cm^{-1}. The TGA measurements were performed on Perkin–Elmer under a nitrogen atmosphere using the heating rate of 10 °C min^{-1} from 80 to 700 °C. The mechanical properties of the dry membranes were measured using SHIMADZU

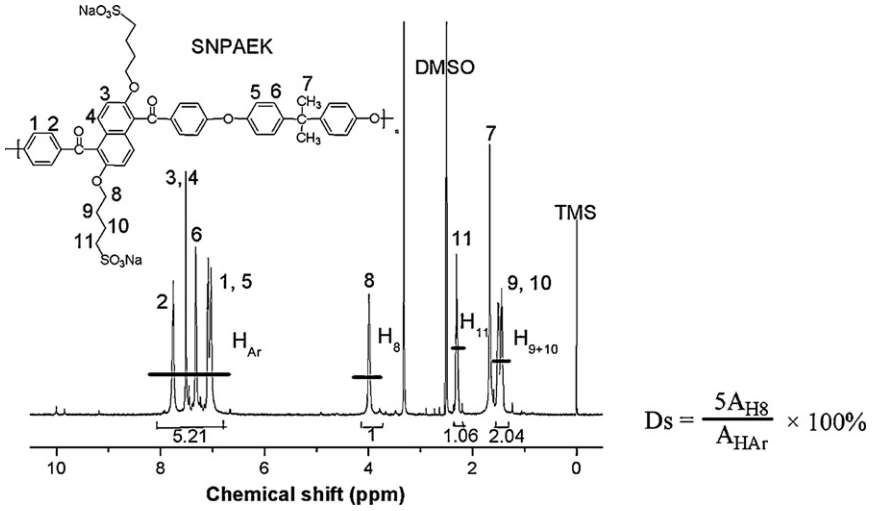

$$Ds = \frac{5A_{H8}}{A_{HAr}} \times 100\%$$

Fig. 1. ^{1}H NMR spectra of SNPAEK.

AG-I 1 KN at the speed of 2 mm min^{-1}. At least five samples (15 mm × 4 mm) were used for each measurement and their average values were calculated.

2.4. Oxidative stability and solubility

Oxidative stability of the SKB-*xx* membranes was evaluated by immersing the films into the Fenton's reagent (3% H_2O_2 containing 2 ppm $FeSO_4$) at 80 °C. After immersing, the membrane samples were collected by filtering and then dried at 120 °C for 10 h in a vacuum oven. We evaluated the degradation of the membranes by the residual weight and the visual observation. The solubility of the SKB-*xx* membranes was evaluated by immersing the films into several organic solvents at room temperature for 1 h. Moreover, the residual membranes after immerging in DMSO at 60 °C for 24 h were filtered and then dried at 120 °C for 10 h in a vacuum oven.

2.5. Ionic exchange capacity (IEC)

The IEC values of these membranes were determined by classical acid–base titration. The membranes in acid form were immersed in 1 M NaCl solutions for 24 h to exchange all the H^+ ions to Na^+ ions. The H^+ ions in solution were then titrated with 0.01 M NaOH using phenolphthalein as indicator. The ion-exchange capacities were calculated from:

$$\text{IEC} = \frac{\text{consumed NaOH(ml)} \times \text{molarity NaOH}}{\text{weight of dry membrane}} (\text{meq. g}^{-1}) \quad (1)$$

2.6. Water uptake and swelling ratio

Before testing water uptake and swelling ratio, the membranes were vacuum-dried at 100 °C until constant weights were obtained. The weight (W_{dry}) and length (L_{dry}) of dry membranes were measured. Then the dried samples were immersed in deionized water for 24 h at different temperatures. After that the samples were taken out and immediately weighed (W_{wet}) and length (L_{wet}) after wiping out the surface water. The water uptake was calculated using the expression:

$$\text{water uptake(WU)(\%)} = \frac{W_{wet} - W_{dry}}{W_{dry}} \times 100 \quad (2)$$

where W_{wet} is the weight of fully hydrated membrane and W_{dry} is the weight of the dry membrane.

Swelling ratio of membranes was calculated with the following formula:

$$\text{swelling ratio(\%)} = \frac{L_{wet} - L_{dry}}{L_{dry}} \times 100 \quad (3)$$

where L_{wet} is the length of fully hydrated membrane and L_{dry} is the length of the dry membrane.

2.7. Proton conductivity and methanol permeability

The in-plane proton conductivity in water-equilibrated membranes was determined by a four-point probe alternating current impedance spectroscopy using an impedance/gain-phase analyzer (Solartron 1260) and an electrochemical interface (Solartron 1287). A single cell with two pairs of gold-plate electrodes was mounted on a Teflon plate and immersed in deionized water where the temperature was controlled. The proton conductivity was calculated by the following equation:

$$\sigma = \frac{L}{R \times S} \quad (4)$$

where σ is the proton conductivity (S cm^{-1}), L is the distance between the two electrodes (L = 1 cm), R is the resistance value of the membrane and S is the cross-section area of the membrane (cm^2).

The methanol permeability was measured by using a two-chamber glass diffusion cell, which was consisted of two identical compartments separated by the test membranes placed on a screw clamp. 10 M methanol solution was placed on one side of the cell

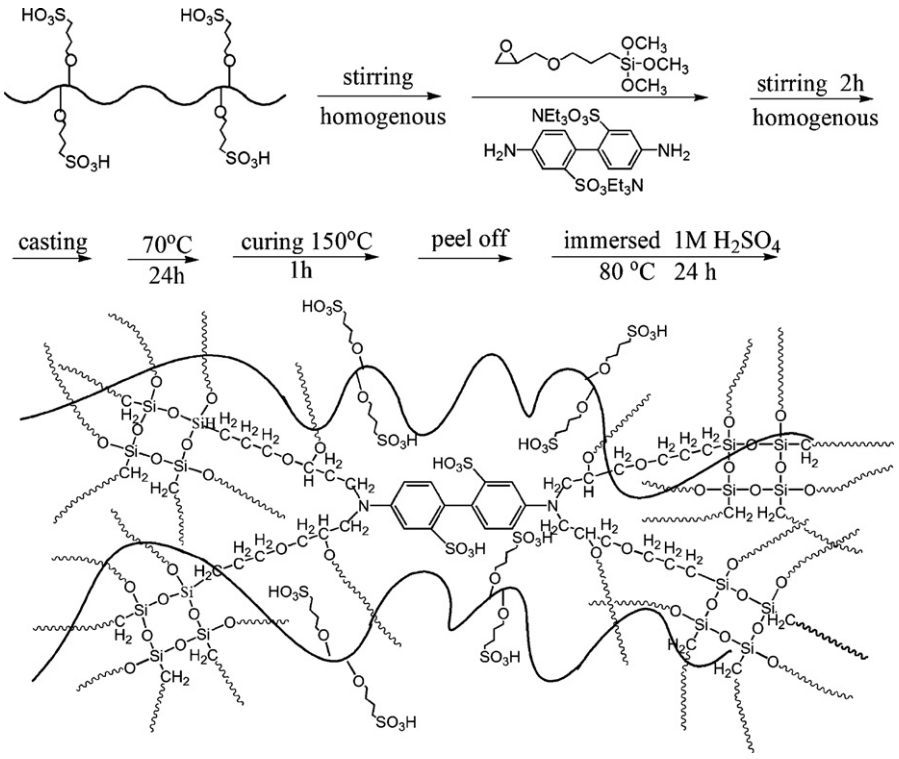

Fig. 2. Scheme for illustrating the preparation of SKB-*xx* hybrid membranes.

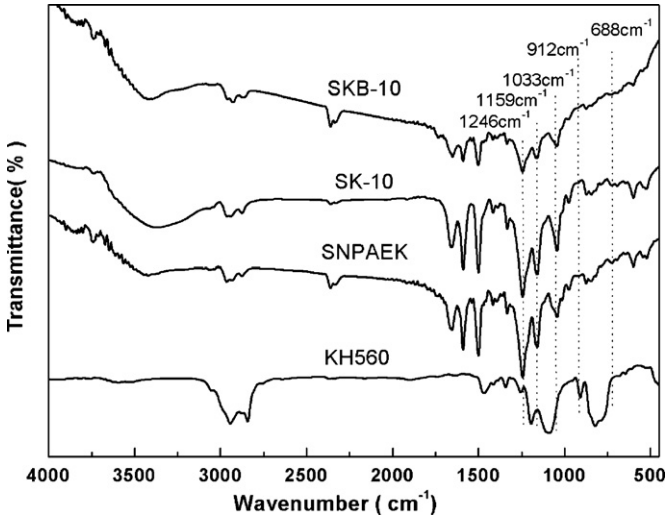

Fig. 3. FT-IR spectra of SKB-*xx* hybrid membranes.

and water was placed on the other side. Each chamber was stirred by a magnetic stirrer to ensure uniformity. The concentration of methanol was determined by using SHIMADZU GC-8A chromatograph. The methanol permeability was calculated as follows:

$$C_B(t) = \frac{A}{V_B}\frac{DK}{L}C_A(t - t_0) \quad (5)$$

where A (cm^2) and L (cm) are the effective area and the thickness of membrane, respectively. V_B (mL) is the volume of diffusion reservoir. C_A and C_B (mol L^{-1}) are the methanol concentration in feed and in diffusion reservoir, respectively. DK (cm^2 s^{-1}) is the methanol permeability.

3. Results and discussion

3.1. Preparation of the SKB-xx membranes

The hybrid SKB-*xx* membranes were prepared via oxirane ring cleavage and sol–gel reaction. The reaction between epoxy of KH-560 and amine group of BDSA via oxirane ring cleavage leaded to the organic polymeric network, while the hydrolysis of Si–$(OR)_3$ catalyzed by H^+ leaded to the cross-linking inorganic siloxane network. The reaction scheme of the hybrid SKB-*xx* membranes is shown in Fig. 2. The hybrid membranes with a mean thickness of 67 μm were brown and transparent indicating good compatibility between the two polymers. FT-IR spectroscopy measurement was used to confirm the cross-linked reaction between the epoxide and amino groups and the formation of polysiloxane network. The FT-IR spectra of SNPAEK, KH-560, SKB-10, as well as SK-10, are shown in Fig. 3. The observed bands at 1246 cm^{-1} and 1033 cm^{-1} were assigned to symmetric and asymmetric stretching vibrations of O=S=O. The infrared band at about 688 cm^{-1} can be assigned to S–O stretching of sulfonated groups. Compared with the spectrum of KH-560, the peak of the epoxy group (912 cm^{-1}) disappeared in the hybrid SKB-10 membrane, which shown that the epoxide ring opened and produced a three-dimensional network. Meanwhile, the appearance of Si–O–Si stretching vibration at 1159 cm^{-1} confirmed the formation of Si–O–Si cross-linked structure.

Table 1
Solubility of SKB-*xx* hybrid membranes in various common organic solvents[a].

Sample	DMSO	DMF	NMP	DMAc	Methanol	Water	Residual weight [b]
SNPAEK	S	S	S	S	S_w	S_w	S
SK-10	S_w	S_w	S_w	S_w	S_w	I	87.21%
SKB-5	S_w	S_w	S_w	S_w	S_w	I	88.54%
SKB-10	S_w	S_w	S_w	S_w	I	I	91.31%
SKB-15	S_w	S_w	I	S_w	I	I	98.28%
SKB-20	I	I	I	I	I	I	99.03%

[a] S: soluble at room temperature. I: insoluble at room temperature. S_w: swelling (or partly dissolved) at room temperature.
[b] The residual weight after 24 h immerged in DMSO at 60 °C.

After hybrid, the SKB-*xx* membranes cannot be dissolved in several organic solvents at room temperature but could be swollen (Table 1), which indicated that the cross-linked networks were successfully incorporated into the SNPAEK membranes. Table 1 shows that the residual weight of the hybrid membranes increased with the KH-560 content, which indicates a increment of the cross-linked density.

3.2. Thermal and mechanical properties

Though the operating temperature is mild for the DMFC, the fabrication of the membrane electrode assemblies still need the membrane material has good thermal property. The thermal stabilities of the membranes were investigated by TGA measurement. The 5% and 10% weight loss temperature ($T_{d5\%}$ and $T_{d10\%}$) of the SNPAEK and SKB-*xx* membranes are listed in Table 2. The $T_{d5\%}$ of the hybrid membranes (above 242 °C) was higher than that of the pristine SNPAEK membrane (230 °C). The cross-linked siloxane network in the hybrid membrane is temperature tolerant and can improve the heat resistance of membranes [30]. Fig. 4 shows the TGA curves of SNPAEK and SKB-*xx* membranes. We can see that all the membranes in acid form contained two step degradation patterns. The first degradation step observed around 220–310 °C was attributed to the elimination of the sulfonic acid groups located on the sulfobutylate side chain and on the BDSA. The second step started at about 460 °C corresponded to the main chain decomposition. The TGA study revealed that the thermal stabilities of the pristine SNPAEK had been improved by the incorporation of the Si–O–Si cross-linked structure into the membrane.

It is essential for PEMs to possess adequate mechanical integrity to withstand the fabrication of the membrane electrode assembly. The mechanical properties of dry SKB-*xx* membranes were measured using a tensile testing instrument at room temperature. The mechanical properties of SKB-*xx* membranes were evaluated

Table 2
Thermal and mechanical properties of the SKB-*xx* hybrid membranes.

Samples	$T_{d5\%}$[a] (°C)	$T_{d10\%}$[b] (°C)	Tensile strength (MPa)	Young's Modulus (MPa)	Elongation at break (%)
SNPAEK	230	252	37 ± 2	797 ± 19	24 ± 4
SK-10	235	248	42 ± 1	876 ± 9	15 ± 2
SKB-5	242	253	40 ± 3	1044 ± 40	21 ± 1
SKB-10	249	260	46 ± 5	1187 ± 22	15 ± 3
SKB-15	259	271	48 ± 2	911 ± 30	12 ± 2
SKB-20	267	282	46 ± 1	1032 ± 17	10 ± 2

[a] Temperature of 5% weight loss.
[b] Temperature of 10% weight loss.

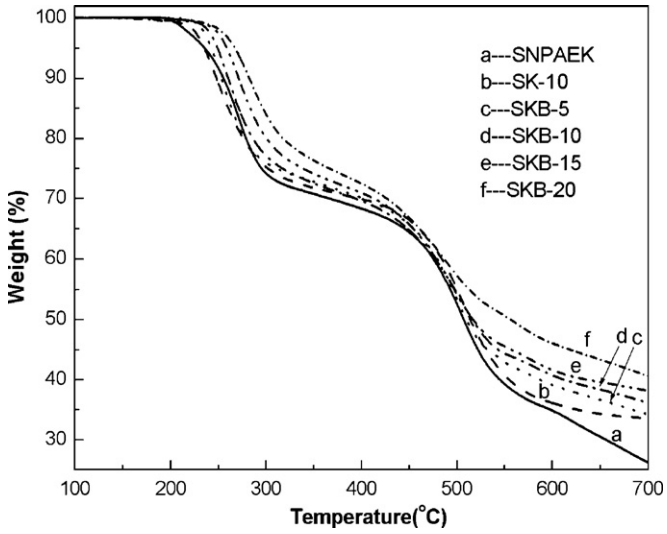

Fig. 4. TGA curves of SKB-*xx* hybrid membranes.

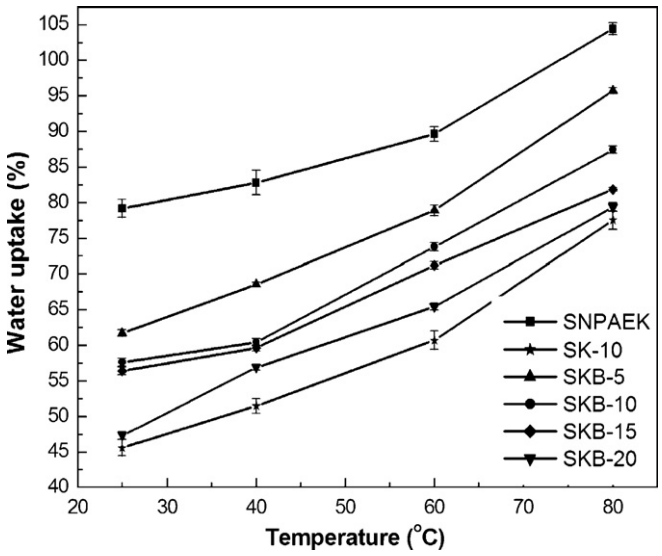

Fig. 5. Water uptake of SKB-*xx* hybrid membranes.

and listed in Table 2. The SKB-*xx* membranes in dry state had tensile stress at maximum load of 40–48 MPa, Young's modulus of 911–1187 MPa and elongation at break of 10–21%. The hybrid membranes showed the improved tensile strength and Young's modulus compared with the pristine SNPAEK membrane. The elongation at break decreased with the introduction of cross linking agent due to the cross-linked network restricted the motion of SNPAEK chain segmental. Compared with the mechanical properties of Nafion117 which had a tensile stress of 38 MPa, a Young's modulus of 180 MPa and a elongation at break 301.5% in the dry state [31], the SKB-*xx* series membranes showed higher tensile strength and Young's modulus but lower elongation at break, which was attributed to the rigid aromatic structure of the polymer chain and the cross-linked network structure. The mechanical properties of SKB-*xx* membranes in dry states showed they were strong and flexible enough to be used as PEMs.

3.3. IEC, water uptake and swelling of the SKB-xx membranes

The IEC value indicates the concentration of sulfonic acid group in the membrane. To get the proper membranes for DMFCs, there must be sufficient IEC value to provide suitable proton conductivity. Table 3 shows the IEC values of SKB-*xx* membranes. With the increasing of KH-560 content, the IEC value decreased from 2.17 to 1.89 meq. g^{-1} gradually. However, with the same weight ratio of KH-560, the IEC value of SKB-10 (2.05 meq. g^{-1}) was higher than that of SK-10 (1.92 meq. g^{-1}), which could be attributed to the additional sulfonic acid groups from BDSA. The additional sulfonic acid groups were also helpful to keep the high proton conductivity in the SKB-*xx* membranes.

The hydrophilic property plays an important role in PEMs. For most of the proton conductive polymer, water acts as the carrier which transports the proton through the membranes. However excessive water uptake would decrease the mechanical properties and increase the methanol permeability of the membranes. Normally, the water uptake depends strongly on the IEC value. Fig. 5 shows that the introduction of KH-560 and BDSA greatly reduces the water uptake of the membranes. This may due to the formation of cross-linked network structure and the slightly reduced IEC value. For example, the water uptake of pristine SNPAEK is 79% and the value of SKB-20 is merely 47% at 25 °C. Similarly, the swelling ratio of the SKB-*xx* membranes was compressed by the cross-linked network too. At 25 °C, the swelling ratio decreased from 21% to 15% with the increasing content of KH-560 (Fig. 6). There are two aspects by the effect of silica and amine groups: (i) a hygroscopic effect due to the silica nodes and inherent amino, which would increase the content of bound water; (ii) a cross-linking effect due to silanol sol–gel polymerization and amine/epoxide linkage, which would reduce the mobility and the free-volume of polymer chains. Also, it could decrease the water uptake and swelling ratio [32]. These results indicated that in the SKB-*xx* hybrid membranes, the cross-linking effect was more prominent than the hygroscopic effect. The properties of the Nafion 117 membrane are also listed in Table 3 for comparison. Though SKB-*xx* membranes showed higher water uptake and swelling ratio than Nafion, their values had been much reduced compared with the pristine membrane and lower than the other kinds of sulfonated aromatic polymers [33,34].

Table 3
Properties of the SKB-*xx* hybrid membranes.

Samples	IEC (meq. g^{-1})	Methanol permeability ($cm^2\ s^{-1}$)	Proton conductivity (10^{-2} S cm^{-1})		Water uptake (%)		Swelling ratio (%)	
			25 °C	80 °C	25 °C	80 °C	25 °C	80 °C
SNPAEK	2.17 ± 0.05	12.11×10^{-7}	10.0 ± 0.1	17.5 ± 0.5	79	104	21	37
SK-10	1.92 ± 0.02	5.43×10^{-7}	7.3 ± 0.3	14.7 ± 0.2	46	78	17	25
SKB-5	2.14 ± 0.01	8.20×10^{-7}	9.3 ± 0.1	19.2 ± 0.2	62	96	18	29
SKB-10	2.05 ± 0.01	4.91×10^{-7}	9.0 ± 0.1	17.9 ± 0.1	58	87	17	27
SKB-15	1.93 ± 0.04	4.82×10^{-7}	7.4 ± 0.1	14.5 ± 0.2	56	82	16	24
SKB-20	1.89 ± 0.06	4.67×10^{-7}	6.6 ± 0.1	12.9 ± 0.1	47	79	15	22
Nafion 117[43]	0.90 ± 0.03	10.05×10^{-7}	7.6 ± 0.1	14.6 ± 0.2	18.3	27.9	10.6	17.2

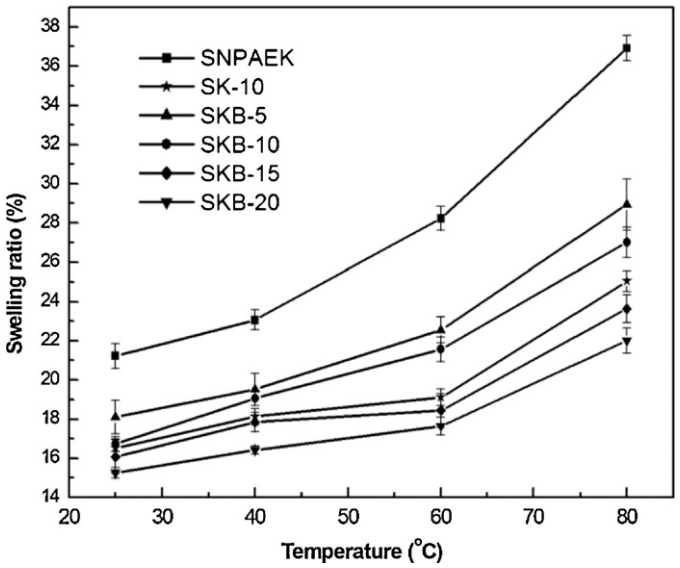

Fig. 6. Swelling ratio of SKB-*xx* hybrid membranes.

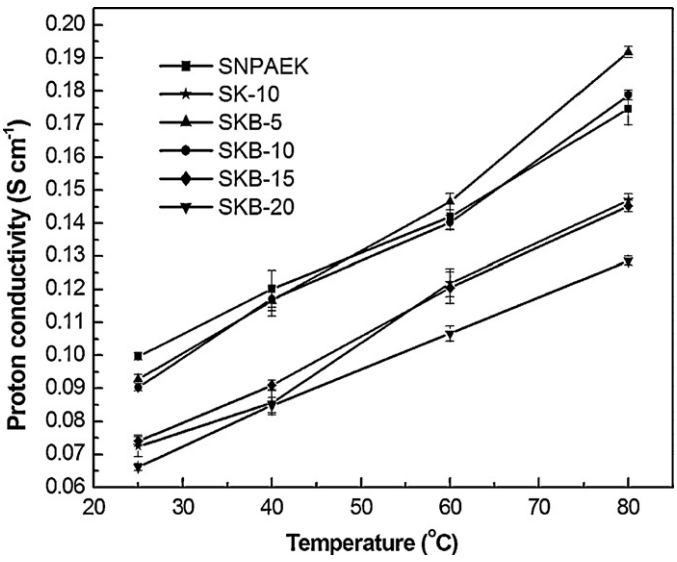

Fig. 8. Proton conductivity of SKB-*xx* hybrid membranes.

3.4. Oxidative stability

Radical species such as HO• and HOO• can arise from reactant diffusion through the membrane and incomplete oxygen reduction. It is known that oxidative attack by HO• and HOO• radicals occurs mainly within the hydrophilic domain to cause the degradation of polymer chain [35]. The mechanical degradation in Fenton's reagent is strongly affected by the amount of sulfonation of the membranes, in general, a higher IEC value leads to lower oxidation stability [36]. The oxidative stability of the SKB-*xx* membranes was calculated in Fenton's reagent at 80 °C. This method is regarded as one of the standard tests to gauge relative oxidative stability and to simulate accelerated fuel cell operating conditions [37]. Fig. 7 shows the residual weight of the hybrid and pristine membranes after immersing in the Fenton's reagent as a function of time. It was found that the SNPAEK membrane began to break into piece by shaking after 35 min. While the SKB-*xx* hybrid membranes showed better oxidation stability than the pristine SNPAEK membrane, which did not break until 156 min. Though the SKB-*xx* series membranes show poorer oxidative stability than Nafion, the oxidative stability of the SKB-*xx* series membranes was increased with the amount of Si–O–Si and epoxy cross-linking structures. There are two reasons: (1) The Si–O–Si structure shows good oxidation stability. (2) The cross-linked network restricts the swelling of the membrane, decreasing the attack opportunity of free radicals in absorbed water.

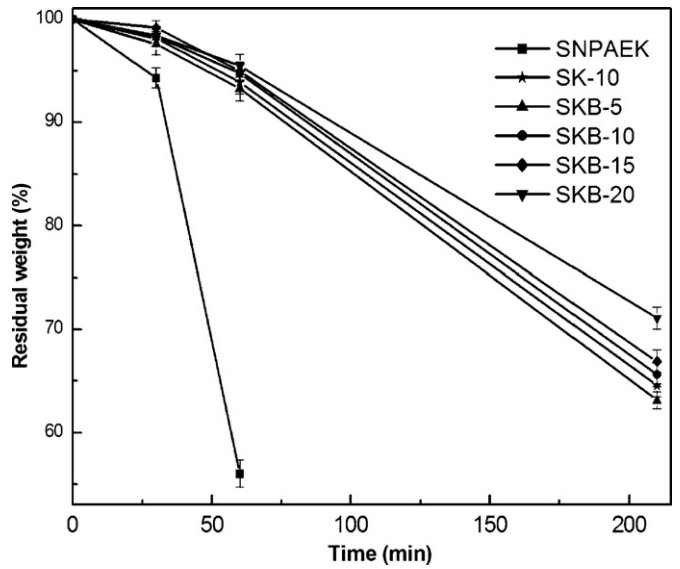

Fig. 7. Oxidative stability of SKB-*xx* hybrid membranes.

3.5. Proton conductivities

The proton conductivities of SKB-*xx* membranes were measured at 100% RH and plotted as functions of temperature (Fig. 8). As expected, the proton conductivities increased with the increasing temperature. All the membranes showed comparable proton conductivity to Nafion 117. For SKB-5, its proton conductivity was 0.192 S cm^{-1} at 80 °C, which was higher than the 0.146 S cm^{-1} of Nafion 117. The results showed that after introducing cross-linked network structure into the SNPAEK membranes, the proton conductivity of the resulting SK-10 membrane decreased to 0.147 S cm^{-1} at 80 °C. This may be due to the introduction of the cross-linker (KH-560), which not only diluted the ion concentration but also hindered the proton transport process since the enhanced compact nature of the membrane. In order to reduce the effect of the cross-linker on decreasing the proton conductivity, BDSA was added into the cross-linked system, which acted as a robust scaffold and also provided the sulfonated groups for conducting protons. As a result, the proton conductivity of SKB-10 still remained 0.179 S cm^{-1} at 80 °C, which was higher than the 0.147 S cm^{-1} of SK-10. From Table 3, we can find that the proton conductivities of SKB-*xx* membranes decreased with the increasing KH-560 content. However, it should be noticed that the proton conductivity of SKB-5 and SKB-10 reached to 0.192 and 0.179 S cm^{-1} at 80 °C, respectively, which was higher than the 0.175 S cm^{-1} of SNPAEK. Actually, the proton conductivity of PEM depended on the proton concentration in membranes [38]. The pristine SNPAEK membrane possessed much higher water content, which may dilute the concentration of the sulfonic acid groups. However, the cross-linked network of SKB-*xx* membranes can tolerate much higher ionic contents without excessive swelling at high temperature. As a result, the SKB-*xx* hybrid membranes exhibited higher concentration of sulfonic acid groups than the pristine SNPAEK membrane with the similar IEC, which may be responsible for their high proton conductivity at high temperature [39,40].

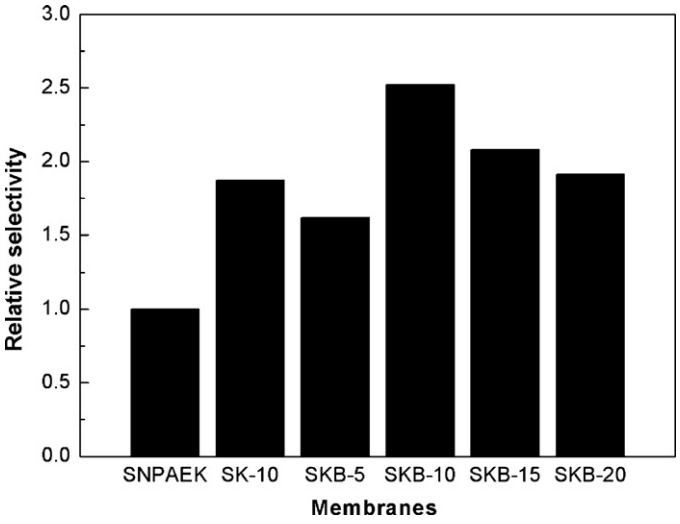

Fig. 9. Relative selectivity of SKB-*xx* hybrid membranes.
Relative selectivity = SKB-*xx* selectivity/SNPAEK selectivity (selectivity = [proton conductivity]/[methanol permeability])

3.6. Methanol permeability and relative selectivity

Membranes used for DMFC must act as an effective barrier to stop methanol permeability from anode to cathode. It has been concluded that methanol is transported by diffusion in the membrane and by convection with the water [41]. So, the methanol permeability increases with the increasing water content, therefore with the Ds. But the influence of the membrane dimensional stability on the methanol permeability should also be taken into account [42]. Table 3 shows the methanol permeability of the SKB-*xx* membranes at room temperature. After cross-linking reaction, the methanol permeability of SKB-*xx* membranes were 4.67×10^{-7}–8.20×10^{-7} $cm^2\ s^{-1}$, which were much lower than that of the SNPAEK (12.11×10^{-7} $cm^2\ s^{-1}$). The results indicated that the formation of cross-linked network can reduce the vacant space where the free water molecules absorbed and introduce a denser structure to act as a methanol barrier. Compared with the Nafion 117(10.05×10^{-7} $cm^2\ s^{-1}$), the rigid aromatic structure and the cross-linked network structure in SKB-*xx* membranes exhibited their advantages in the resistance of methanol crossover.

The selectivity is the ratio of proton conductivity to the methanol permeability, which is often used to evaluate the potential performance of DMFC membranes. Fig. 9 shows that the selectivity of all the hybrid membranes was higher than the pristine SNPAEK membrane. SKB-10 showed the highest selectivity which was as much as 2.5 times than the SNPAEK. The results suggested that the SKB-*xx* hybrid membranes could be applied as potential PEM materials for DMFCs.

4. Conclusion

A novel type of organic–inorganic hybrid PEMs containing sulfonated cross-linked polysiloxanes was successfully prepared by sol–gel and cross-linking reaction. The SNPAEK/KH-560/BDSA hybrid membranes showed excellent solvent resistance, thermal and mechanical stability. The oxidative stability of the hybrid membranes was much improved by the cross-linked network structure. The water uptake and swelling ratio were also reduced by the cross-linking effect. Furthermore, the SKB-*xx* membranes showed excellent proton conductivities. For example, both of the SKB-5 ($0.192\ S\ cm^{-1}$) and SKB-10 ($0.179\ S\ cm^{-1}$) showed higher proton conductivities than the pristine SNPAEK ($0.175\ S\ cm^{-1}$) at 80 °C. Meanwhile, the methanol permeability was also much reduced by introducing the cross-linked network structure in the membrane. All the results indicated the introduction of sulfonated cross-linked polysiloxanes network can significantly improve the performance of the SNPAEK materials in DMFCs.

Acknowledgements

This work was supported by the China High-Tech Development 863 Program (Grant No. 2007AA03Z218) and National Natural Science Foundation of China (Grant No. 21074044) and Science and Technology Development Plan of Jilin Province (Grant No. 20100110).

References

[1] M.A. Hickner, H. Ghassemi, Y.S. Kim, B.R. Einsla, J.E. McGrath, Chem. Rev. 104 (2004) 4587–4612.
[2] V. Neburchilov, J. Martin, H.J. Wang, J.J. Zhang, J. Power Sources 169 (2007) 221–238.
[3] A. Heinzel, V.M. Barragan, J. Power Sources 84 (1999) 70–74.
[4] H. Hou, G. Sun, Z. Wu, W. Jin, Q. Xin, Int. J. Hydrogen Energy 33 (2008) 3402–3409.
[5] P.X. Xing, G.P. Robertson, M.D. Guiver, S.D. Mikhailenko, K.P. Wang, S. Kaliaguine, J. Membr. Sci. 229 (2004) 95–106.
[6] B. Bae, K. Miyatake, M. Watanabe, Macromolecules 43 (2010) 2684–2691.
[7] C. Bonis, A. D'Epofanio, M.L.D. Vona, B. Mecheri, E. Traversa, M. Trombetta, S. Licoccia, J. Polym. Sci. Part A: Polym. Chem. 48 (2010) 2178–2186.
[8] M.J. Robb, D.M. Knauss, J. Polym. Sci. Part A: Polym. Chem. 47 (2009) 2453–2461.
[9] T. Suda, K. Yamazaki, H. Kawakami, J. Power Sources 195 (2010) 4641–4646.
[10] K.D. Kreuer, J. Membr. Sci. 185 (2001) 29–39.
[11] D.S. Kim, G.P. Robertson, M.D. Guiver, Macromolecules 41 (2008) 2126–2134.
[12] T.B. Norsten, M.D. Guiver, J. Murphy, T. Astill, T. Navessin, S. Holdcrof, B.L. Frankamp, V.M. Rotello, J. Ding, Adv. Funct. Mater. 16 (2006) 1814–1822.
[13] K. Shao, J. Zhu, C.J. Zhao, X.F. Li, Z.M. Cui, Y. Zhang, H.T. Li, D. Xu, G. Zhang, T.Z. Fu, J. Wu, H. Na, W. Xing, J. Polym. Sci. Part A: Polym. Chem. 47 (2009) 5772–5783.
[14] S.D. Mikhailenko, K. Wang, S. Kaliaguine, P.X. Xing, G.P. Robertson, M.D. Guiver, J. Membr. Sci. 233 (2004) 93–99.
[15] K.S. Roelofs, A. Kampa, T. Hirth, T. Schiestel, J. Appl. Polym. Sci. 6 (2009) 2998–3009.
[16] Y. Gao, G.P. Rpbertson, M.D. Guiver, X.G. Jian, S.D. Mikhailenko, K.P. Wang, S. Kaliaguine, J. Polym. Sci. Part A: Polym. Chem. 41 (2003) 2731–2742.
[17] Y. Gao, G.P. Robertson, M.D. Guiver, X.G. Jian, J. Polym. Sci. Part A: Polym. Chem. 41 (2003) 497–507.
[18] K. Xu, C. Chanthad, M.R. Gadinski, M.A. Hicker, Q. Wang, Appl. Mater. Interfaces 11 (2009) 2573–2579.
[19] L.J. Su, L. Li, H. Li, J.K. Tang, Y.M. Zhang, W. Yu, C.X. Zhou, J. Power Sources 194 (2009) 220–225.
[20] H. Ahmad, S.K. Kamarudin, U.A. Hasran, W.R.W. Daud, Int. J. Hydrogen Energy 35 (2010) 2160–2175.
[21] W.F. Chen, P.L. Kuo, Macromolecules 40 (2007) 1987–1994.
[22] H. Zou, S.S. Wu, J. Shen, Chem. Rev. 108 (2008) 3893–3957.
[23] T.Z. Fu, Z.M. Cui, S.L. Zhong, Y.H. Shi, C.J. Zhao, G. Zhang, K. Shao, H. Na, J. Power Sources 185 (2008) 32–39.
[24] D. Gomes, R. Marschall, S.P. Nunes, M. Wark, J. Membr. Sci. 322 (2008) 406–415.
[25] J. Wu, Z.M. Cui, C.J. Zhao, H.T. Li, Y. Zhang, T.Z. Fu, H. Na, W. Xing, Int. J. Hydrogen Energy 34 (2009) 6740–6748.
[26] M. Lavorgna, M. Gilbert, L. Mascia, G. Mensitieri, G. Scherillo, G. Ercolano, J. Membr. Sci. 330 (2009) 214–226.
[27] J. Zhu, K. Shao, G. Zhang, C.J. Zhao, Y. Zhang, H.T. Li, M.M. Han, H.D. Lin, D. Xu, H.B. Yu, H. Na, Polymer 51 (2010) 3047–3053.
[28] P.X. Xing, G.P. Robertson, M.D. Guiver, S.D. Mikhailenko, S. Kaliaguine, J. Polym. Sci. Part A: Polym. Chem. 42 (2004) 2866–2876.
[29] Z.Q. Shi, S. Holdcroft, Macromolecules 38 (2005) 4193–4201.
[30] L. Honma, O. Nishikawa, T. Sugimoto, S. Nomura, H. Nakajima, Fuel Cell 2 (2002) 52–58.
[31] B. Liu, G.P. Robertson, D.S. Kim, M.D. Guiver, W. Hu, Z.H. Jiang, Macromolecules 40 (2007) 1934–1944.
[32] R.Q. Fu, J.J. Woo, S.J. Seo, J.S. Lee, S.H. Moon, J. Power Sources 179 (2008) 458–466.
[33] Y. Gao, G.P. Robertson, M.D. Guiver, X.G. Jian, S.D. Mikhailenko, S. Kaliaguine, Solid State Ionics 176 (2005) 409–415.
[34] P.X. Xing, G.P. Robertson, M.D. Gover, S.D. Mikhailenko, S. Kaliaguine, J. Polym. Sci. Part A: Polym. Chem. 42 (2004) 2866–2876.
[35] J.H. Pang, H.B. Zhang, X.F. Li, L.F. Wang, B.J. Liu, Z.H. Jiang, J. Membr. Sci. 318 (2008) 271–279.
[36] X.Y. Shang, D. Shu, S.J. Wang, M. Xiao, Y.Z. Meng, J. Membr. Sci. 291 (2007) 140–147.

[37] P.X. Xing, G.P. Robertson, M.D. Guiver, S.D. Mikhailenko, S. Kaliaguine, Macromolecules 37 (2004) 7960–7967.
[38] E.M.W. Tsang, Z. Zhang, Z. Shi, T. Soboleva, J. Am. Chem. Soc. 129 (2007) 15106–15107.
[39] K.D. Kreuer, S.J. Paddison, E. Spohr, M. Schuster, Chem. Rev. 104 (2004) 4637–4678.
[40] T.J. Peckham, J. Schmeisser, M. Rodgers, S. Holdcroft, J. Mater. Chem. 17 (2007) 3255–3268.
[41] F. Meier, S. Denz, A. Weller, G. Eigenberger, Fuel Cells 3 (2003) 161.
[42] F. Meier, J. Kerres, G. Eigenberger, J. Membr. Sci. 241 (2004) 137–141.
[43] H.D. Lin, C.J. Zhao, W.J. Ma, H.T. Li, H. Na, J. Membr. Sci. 345 (2009) 242–248.